

# A High-Performance Miniaturized Wideband Active Electric Probe Design

xdhan2002

December 2024

## Abstract

In this letter, a miniaturized active electric probe, which simultaneously achieves high performance in terms of wide bandwidth, high spatial resolution, and high sensitivity, is proposed for radiation source localization. This probe is manufactured utilizing a printed circuit board (PCB) process, occupying a compact area of 588 mm<sup>2</sup>. High spatial resolution is achieved through an ultra-narrow induction tip with an effective width of 0.1 mm, the PCB process limit. Sensitivity is improved by integrating an amplification circuit with a 17 dB gain. Wide bandwidth is achieved by implementing a wideband amplifier of 10 MHz to 27.8 GHz and a horizontal tapered substrate integrated coaxial line transition structure. Through the measurement results, the proposed probe can operate from 10 MHz to 27.8 GHz. At 27.8 GHz, the spatial resolution of the proposed probe is 0.41 mm. The sensitivity has a 17 dB improvement compared with the reference passive probe

**Index Terms** — **Amplifier, electric probe, high sensitivity, high spatial resolution, horizontal substrate integrated coaxial line (SICL) transition.**

# 1 Introduction

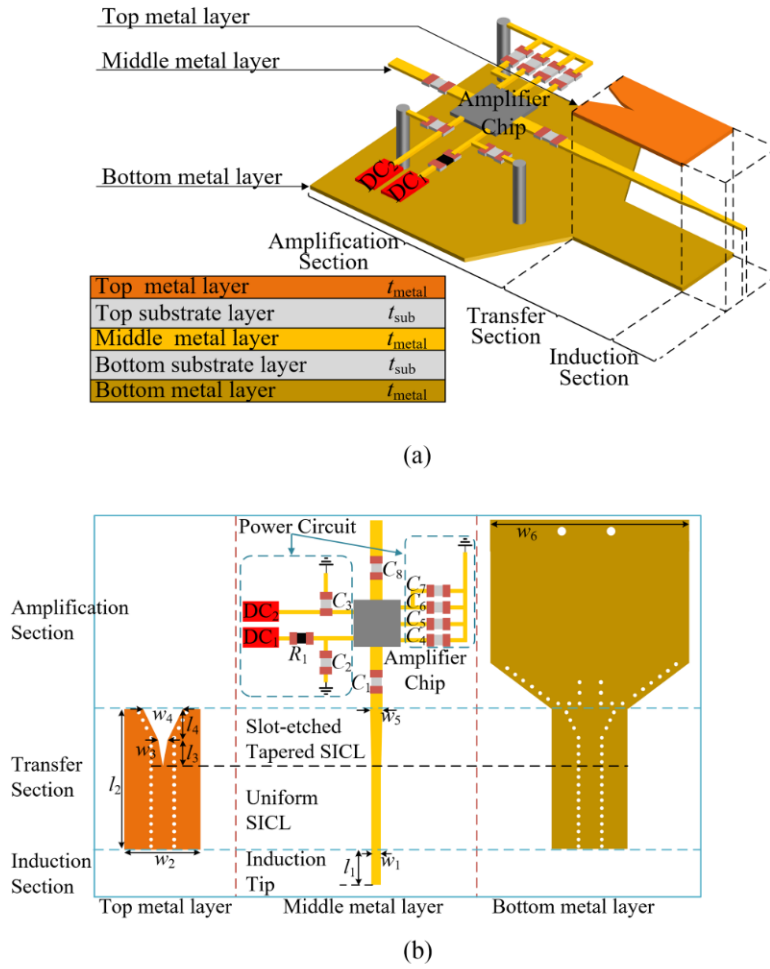
AS THE development of miniaturization, high-density and low-power ICs are being made, the issue of electromagnetic interference (EMI) is becoming increasingly prevalent [1]. The near-field scanning technology, which allows for real-time analysis and diagnosis of EMI problems without requiring knowledge of the internal structure of the chips, has gained significant research interest in recent years [2], [3], [4], [5]. Electric probes, as crucial components in near-field scanning of electric fields, must simultaneously possess wide bandwidth, high spatial resolution, and high sensitivity. According to whether the electric probe contains active components, it can be categorized into the passive probe and active probe.

As for the passive electric probe, it typically comprises three main sections, namely, the induction section, the transfer section, and the output section [6], [7], [8], [9], [10]. According to Maxwell's displacement current principle, the induction tip structure in the induction section can detect external electric fields and generate a current source within the probe. The induced current signal will encounter impedance discontinuities from the transfer section to the output section, which restricts the probe's bandwidth. To address the issue of discontinuities, a vertical transition formed by coaxial-through-hole via array [7], [8], [9], [10] was adopted as the replacement for a single via [6]. However, this approach also has bandwidth limitations because the parasitic capacitance and inductance of the via array have a negative impact on the high-frequency performance of the probe. The other approach to enhance the operating frequency is reducing the induction tip width [11], which simultaneously improves the spatial resolution while reducing the sensitivity. Therefore, there is a trade-off relationship between the spatial resolution and sensitivity of passive electric probes [12].

This letter proposes a high-performance miniaturized wideband active electric probe for radiation source localization in near-field measurement. The probe features an ultra-narrow induction tip width of 0.1 mm, enabling superior spatial resolution. The integration with an amplification circuit with 17 dB gain enhances the sensitivity. The design employs a wideband amplifier in conjunction with a horizontal substrate integrated coaxial line (SICL) transition to achieve a wide bandwidth. The induced signal is transmitted from the induction tip to the amplifier through a SICL and its horizontal transition with excellent impedance matching over a wide frequency band. Leveraging the printed circuit board (PCB) fabrication process, the total area of the manufactured probe is only 588 mm<sup>2</sup>. Experimental results indicate that the bandwidth of the proposed probe ranges from 10 MHz to 27.8 GHz. Notably, the spatial resolution is 0.6 mm at 1 GHz, 0.48 mm at 15 GHz, and 0.41 mm at 27.8 GHz. Furthermore, the sensitivity of the proposed probe is significantly higher, by 17 dB, compared to a passive reference probe lacking the amplification circuit.

## 2 DETAILED DESIGN OF THE PROPOSED ELECTRIC PROBE

The proposed active electric probe is manufactured under the multilayer PCB process. Rogers 4360G2, with a relative permittivity of 6.15, is used as the substrate material. Meanwhile, copper is used as the metal material. The thicknesses of the two substrate layers,  $t_{\text{sub}}$ , are both 0.2 mm, and those of the three metal layers,  $t_{\text{metal}}$ , are all 0.018 mm.

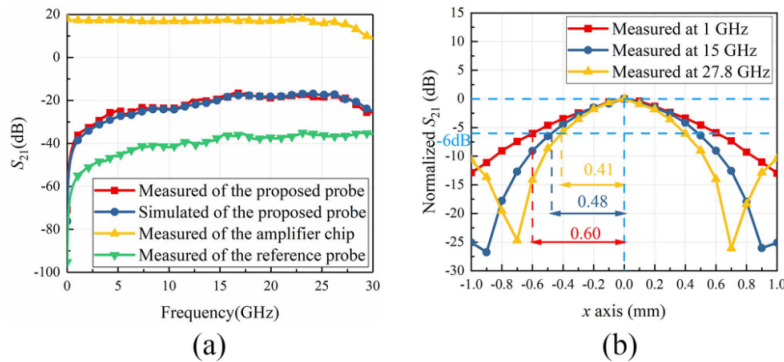


The detailed design of the proposed active electric probe is illustrated in Fig. 1, which showcases its structure and features. Fig. 1(a) displays the three-dimensional structure of the probe, which includes an induction section, a transfer section, and an amplification section. Meanwhile, the stack-up structure

highlights the presence of three metal layers and two substrate layers. Fig. 1(b) provides a 2-D view of each metal layer to better represent the structural characteristics.

The induction section features an induction tip, which detects the external electric field and forms a corresponding current signal. The width  $w_1$  of the induction tip is miniaturized to the PCB process limit to achieve higher spatial resolution. The transfer section comprises a uniform SICL and a horizontal transition formed by the slot-etched tapered SICL. The tapered slot parameters  $w_3$ ,  $w_4$ ,  $l_3$ , and  $l_4$  are designed to minimize the insertion loss and maximize the return loss of the horizontal transition. The width  $w_5$  is designed for the  $50\ \Omega$  characteristic impedance of the microstrip line. The amplification section integrates an amplifier chip, a power circuit, and several ground vias. The amplifier chip is chosen as ADL9005 provided by ADI company, which boasts a gain of 17 dB within the frequency range of 10 MHz to 27.8 GHz. The power circuit contains two DC pads (DC1 and DC2), one resistor (R1), and eight capacitors (C1-C8). As specified in the chip manual, the input and output ports of the amplifier chip are internally matched to  $50\ \Omega$ , and the two bias voltage pins dc1 and dc2 are connected to 5 V and 8.5 V, respectively. The bias resistor R1 ( $300\ \Omega$ ) sets the total current to 80 mA. Two dc blocking capacitors C1 and C8, both with a capacitance of  $0.1\ \mu\text{F}$ , are used to filter out the dc components in the input and output signals. The capacitors C2 and C3, selected as 100 pF and  $0.01\ \mu\text{F}$ , are applied to reduce the bias voltage pulsation. Four capacitors C4-C7 (100 pF,  $0.01\ \mu\text{F}$ ,  $4.7\ \mu\text{F}$ , and  $4.7\ \mu\text{F}$ ), are used to provide low-frequency decoupling for the ac grounding pins of the chip.

### 3 SIMULATION AND MEASUREMENT VALIDATION



A microstrip line is utilized as the device under test (DUT) to evaluate the probe characteristics. The schematic diagram and photography of the experi-

mental setup, as depicted in Fig. 2, show that the DUT is attached to a  $50\ \Omega$  matching load and the source port of a vector network analyzer (VNA), respectively. The proposed active electric probe is attached to the receiving port of the VNA and at a height of 0.5 mm above the DUT. The power source provides 5 V and 8.5 V for dc1 and dc2 in the power circuit. The top and bottom views of the manufactured active electric probe are shown in Fig. 2(a). The calibration factor (CF) can be calculated from the simulated electric field strength  $E_z$  above the center of the calibration device and the measured voltage output  $V_{eout}$  of the probe. According to [4]

$$CF = \frac{E_z}{|V_{eout}|} \quad (1)$$

In the experiment, the signal generator with the output power of 0 dBm is adopted as the signal source to excite the calibration device, which is chosen as a microstrip line. The output voltage  $V_{eout}$  is measured by the spectrum analyzer, as shown in Fig. 3(d). The electric field strength  $E_z$  is simulated utilizing full-wave simulation software, as shown in Fig. 3(e). The result of CF is shown in Fig. 3(f).

## 4 Conclusion

A novel miniaturized active electric probe design is proposed, which simultaneously achieves high performance in terms of wide bandwidth, high spatial resolution, and high sensitivity. The design features a horizontal tapered SICL transition structure, in addition to a wideband amplifier, to attain the desired wide bandwidth. The high spatial resolution is achieved through the design of an ultra-narrow induction tip with an effective width of 0.1 mm, which reaches the PCB process limit. The sensitivity is enhanced by the integration of an amplifier chip with a 17 dB gain and the corresponding power circuit. The measurement results demonstrate that the proposed probe exhibits a bandwidth spanning from 10 MHz to 27.8 GHz, a spatial resolution of 0.6 mm at 1 GHz, 0.48 mm at 15 GHz, and 0.41 mm at 27.8 GHz, and a 17 dB improvement in sensitivity in comparison with the reference passive probe.

## References

- [1] M. Ramdani et al., "The electromagnetic compatibility of integrated circuits," *IEEE Trans. Electromagn. Compat.*, vol. 51, pp. 78–100, 2009.
- [2] S. Liu et al., "Field coupling mechanism investigation," *IEEE Trans. Instrum. Meas.*, vol. 71, 2022.
- [3] J. Wang et al., "Near-field precision measurement system," *IEEE Trans. Instrum. Meas.*, vol. 70, 2021.

- [4] X. He, X.-C. Li, Z.-H. Peng, Y.-X. Liu, and J.-F. Mao, "An ultrawideband magnetic probe with high electric field suppression ratio," *IEEE Trans. Instrum. Meas.*, vol. 70, 2021, Art. no. 8005309.
- [5] Y. Liu, X. Li, Z. Peng, X. He, and J. Mao, "A pair of parallel differential magnetic-field probes with high measurement accuracy and high electric field suppression ratio," *Int. J. RF Microw. Comput.-Aided Eng.*, vol. 31, no. 1, Jan. 2021, Art. no. e22478.
- [6] G. Li, K. Itou, Y. Katou, N. Mukai, D. Pommerenke, and J. Fan, "A resonant E-field probe for RFI measurements," *IEEE Trans. Electromagn. Compat.*, vol. 56, no. 6, pp. 1719–1722, Dec. 2014.
- [7] Z. Yan, J. Wang, W. Zhang, Y. Wang, and J. Fan, "A miniature ultrawideband electric field probe based on coax-thru-hole via array for near-field measurement," *IEEE Trans. Instrum. Meas.*, vol. 66, no. 10, pp. 2762–2770, Oct. 2017.
- [8] W. Liu, Z. Yan, J. Wang, X. Yan, and J. Fan, "An ultrawideband electric probe based on U-shaped structure for near-field measurement from 9 kHz to 40 GHz," *IEEE Antennas Wireless Propag. Lett.*, vol. 18, no. 6, pp. 1283–1287, Jun. 2019.
- [9] J. Wang, Z. Yan, W. Liu, D. Su, and X. Yan, "A novel tangential electric-field sensor based on electric dipole and integrated balun for the nearfield measurement covering GPS band," *Sensors*, vol. 19, no. 9, 2019, Art. no. 1970.
- [10] Z. He, L. Wang, L. Chen, R. Luo, and Q. H. Liu, "A wideband tangential electric field probe and a new calibration kit for near-field measurements," *IEEE Trans. Microw. Theory Techn.*, vol. 70, no. 7, pp. 3557–3565, Jul. 2022.
- [11] S. Jarrix, T. Dubois, R. Adam, P. Nouvel, B. Azais, and D. Gasquet, "Probe characterization for electromagnetic near-field studies," *IEEE Trans. Instrum. Meas.*, vol. 59, no. 2, pp. 292–300, Feb. 2010.